Available online at www.sciencedirect.com
ScienceDirect
Journal of the European Ceramic Society 30 (2010) 1699–1706
www.elsevier.com/locate/jeurceramsoc

Synthesis of nano-crystalline apatite type electrolyte powders for solid oxide fuel cells

E. Jothinathan *, K. Vanmeensel, J. Vleugels, O. Van der Biest

Department of Metallurgy and Materials Engineering, KU Leuven, Kasteelpark Arenberg 44, B-3001 Leuven, Belgium

Received 13 August 2009; received in revised form 4 December 2009; accepted 4 January 2010
Available online 25 January 2010

Abstract

Rare earth silicates with apatite structure are being actively studied as an alternative electrolyte material for solid oxide fuel cells (SOFC) operating in the intermediate temperature range. In this paper we report on the synthesis of $La_{9.33+x/3}Al_xSi_{6-x}O_{26+\delta}$ (with $x = 0$–1.5) and $La_{9.83}Fe_{1.5}Si_{4.5}O_{26}$ powders using a modified sol–gel process. The parameters involved in the process have been optimized for preparing phase pure, homogeneous and nanometer sized powders. The obtained powders were characterized using scanning electron microscopy, X-ray diffraction and thermal analysis. Pressureless sintering experiments were performed and pellets having relative densities greater than 96% could be obtained after 5 h dwelling in the temperature range between 1500 and 1550 °C.

Keywords: Apatite type lanthanum silicates; Solid oxide fuel cell; Modified sol–gel; Nanopowder; Sintering temperature

1. Introduction

Solid oxide fuel cells (SOFC) belong to the class of fuel cells that are generally known to operate at high temperatures (800–1000 °C). The high degradation rate and material cost incurred at temperatures in excess of 900 °C, however, make fuel cells operating at high temperature economically more unfavourable.[1] Lowering of the operating temperature necessitates the need for new electrolyte materials, which have the required oxygen ion conductivity at the operating temperature.

In recent years, rare earth silicates with apatite structure are actively studied as an alternative electrolyte material for SOFC due to their high oxygen ion conductivity in the intermediate temperature. Preparation of these powders using conventional solid-state syntheses were reported widely.[2–5] Although successful in the preparation of high quality powders, the solid-state reaction requires high temperature treatments to achieve single-phase materials.[6] As result of the high temperature treatments, solid-state synthesised powders are relatively coarse (5–10 μm) and long sintering cycles at elevated temperatures are required to densify them.[7,8] Low temperature synthesis not only reduces the cost involved in the processing but also helps in problems like volatilisation when volatile materials are involved in the composition.[9] Tao and Irvine were the first to report the preparation of apatite type lanthanum silicates using the sol–gel technique.[10] Following the report of Tao and Irvine,[10] sol–gel synthesis and other low temperature synthesis of the undoped lanthanum silicates have been reported in literature.[11–17] The fine particle size that results due to the low temperatures employed in the synthesis helps in reducing the sintering temperature required to obtain a material with closed porosity. The sol–gel technique has been successful in reducing the sintering and dwell times in the case of undoped silicates.[12]

Abram and Takeda have shown that substituting Al^{3+} for Si^{4+} in the SiO_4 tetrahedra of the oxyapatite structure increases its ionic conductivity.[18,19] Doping with aluminium increases the conductivity but sintering to full density requires high temperatures and/or dwell times as compared to undoped silicates.[20–25] To the best of our knowledge there has been only one report on the attempts to process aluminium doped lanthanum silicates, using both mechanical alloying and the Pechini method.[20] Impurity formation and hindrance in the formation of the apatite phase, due to a low reactivity even at temperatures up to 1200 °C, however, are reported for Pechini type process.[20] The sintering behaviour of the doped apatite powders, as compared to their undoped variants, has not been evaluated so far.

* Corresponding author. Tel.: +32 16 32 11 92; fax: +32 16 32 19 92.
E-mail address: Ezhil.jothinathan@mtm.kuleuven.be (E. Jothinathan).

0955-2219/$ – see front matter © 2010 Elsevier Ltd. All rights reserved.
doi:10.1016/j.jeurceramsoc.2010.01.003

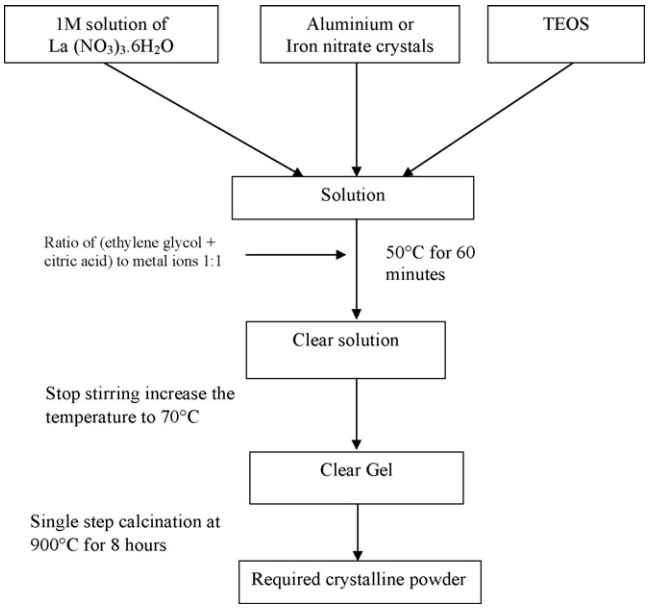

Fig. 1. Outline of the process used in the preparation of doped and undoped lanthanum silicates.

In this paper we report on the synthesis of $La_{9.83}Al_{1.5-x}Si_{4.5+x}O_{26+\delta}$ labelled as LASO-0, LASO-1 and LASO-2, for $x=0$, $x=0.5$ and $x=1$ respectively, and $La_{9.83}Fe_{1.5}Si_{4.5}O_{26+\delta}$ (LFSO), both using the modified sol–gel process. Undoped silicate $La_{9.33}Si_6O_{26}$ (LSO) was also synthesised by the same route and used as a reference powder composition. All five compositions prepared are characterized and their sintering behaviours were evaluated. It is shown that, using the modified sol–gel process, nanometer sized powders can successfully be prepared thereby reducing their sintering temperature and making them appropriate electrolyte candidate materials for intermediate temperature SOFC applications.

2. Experimental procedure

2.1. Powder preparation

Lanthanum nitrate hexa hydrate (99+%, Chempur), aluminium and iron nitrate nano hydrate (98+%, Chempur), tetraethyl orthosilane (98%, Acros Organics), citric acid (Analysis quality, Vel Chemicals) and ethylene glycol (Analysis quality, Vel Chemicals) were used as the starting materials. In order to avoid water absorption by the highly hygroscopic lanthanum nitrate crystals, a one molar solution of lanthanum nitrate is prepared using technical ethanol (~97% ethanol, 3% ether and traces of water as supplied by Univar). The steps involved in the powder preparation are explained below and are schematically shown in Fig. 1.

1. The calculated amount, as dictated by the stoichiometry of the apatite composition, of the one molar lanthanum nitrate hexa hydrate solution is taken.
2. In the case of doped silicates, the required amounts of aluminium or iron nitrate crystals are added to the above solution. The mixture is mixed using a magnetic stirrer until a clear solution is obtained. This step is not required in the case of undoped silicates.
3. Tetraethyl orthosilane (TEOS), the source of silicon is added to the above mixture and stirred till the mixture forms a clear solution again.
4. Ethylene glycol (EG) and citric acid (CA) are added to the above solution. EG and CA together are addressed as gelling agents (GA). The ratio of the gelling agents (EG (moles) + CA (moles) ratio 1:1) to the total number of metal ion moles equals one (referred to as R_g in the text). The mixture is continuously stirred and the temperature of the stirring bath is increased to 50 °C. The mixture is magnetically stirred at this temperature for 60 min.
5. After 60 min the stirring is stopped and the temperature is increased to 70 °C, while this temperature is maintained until the clear solution transforms into a gel.
6. Once the gel is formed, it is calcined in air at 900 °C for 8 h, applying a heating and cooling rate of 20 °C/min down to room temperature.

The time required for gelation varies with the yield required. The gelation time is approximately 4 h for a powder yield of 70 g (100 g of gel on calcination yields 60 g of powder). Fig. 1 summarizes the powder preparation process.

2.2. Characterization studies

To determine the lowest possible calcination temperature, the obtained gels were analyzed using thermogravimetric analysis (TGA). All TGA measurements (DTA 1600 TA Instruments, USA) were performed under flowing oxygen at a rate of 100 ml/min, up to a temperature of 1000 °C with an applied heating rate of 5 °C/min. XRD analysis of the calcined powders was carried out on a *Seifert-3003* equipment in order to determine the phase purity and crystal structure. Measurements were performed using Cu-Kα radiation (40 kV to 40 mA) within the 2θ range of 20–80° using a step size of 0.02° (2θ) and an acquisition time of 2 s. Microstructures of the powder and sintered pellets were examined by scanning electron microscopy (SEM, XL30-FEG, Philips, Eindhoven), equipped with an energy dispersive analysis system (EDS, EDAX) for compositional analysis. Particle size measurements were done after de-agglomeration (powder suspension was subjected to 15 min magnetic stirring followed by 10 min of ultrasound treatment before measurement) using the Mastersizer equipment (Malvern Instruments, UK) and dilatometry studies (NETZSCH DIL 402C, Germany) were carried out on cold pressed powder pellets. The densities of the sintered samples were measured in ethanol using the Archimedes principle.

3. Results and discussion

3.1. Powder preparation

Powders that were prepared using the lanthanum nitrate hexa hydrate ($La(NO_3)_3{\cdot}6H_2O$) salt in as received form, resulted in a

lower lanthanum stoichiometry than desired in the composition. This is attributed to the hygroscopic nature of the lanthanum salt, which inhibits its direct use in the preparation of the starting powders. The problem can be essentially overcome by dissolving the lanthanum nitrate crystals in a suitable solvent.

Three different solvents namely, (1) de-mineralised water, (2) technical ethanol and (3) absolute ethanol were used for dissolving the lanthanum nitrate salt. The influence of these solvents on the phase composition and particle size will be discussed. In all cases a one molar solution of the lanthanum nitrate salt was used to prepare the powders. Inductive coupled plasma atomic emission spectroscopy (ICP-AES) measurements were carried out on this solution in order to determine the exact amount of lanthanum. Based on the ICP-AES measurements, the required amount of La salt solution, as dictated by the stoichiometry of the envisaged powder composition, was taken. Since the aluminium and iron nitrate salts did not exhibit any hygroscopic behaviour, these salts were directly added to the lanthanum nitrate solution. All powders were prepared according to the procedure described in the flowchart shown in Fig. 1. Only, the LASO-0 composition, having the amount of gelling agents to metal ions fixed at one, was investigated to study the influence of the three solvents.

When water was used as the solvent the prepared powders contained secondary phases, mainly La_2O_3 in addition to the desired apatite phase. Fig. 2 shows the X-ray diffraction pattern of the powder prepared with water as the solvent. It is proposed that, due to the immiscibility of the silicon alkoxide (TEOS) and water, the silicon source is not completely incorporated into the gel, so the stoichiometry of the gel differs from the envisaged one and lanthanum rich phases crystallise separately on calcination.

When ethanol, either the technical or absolute grade, was used to dissolve the lanthanum salt, phase pure powders were obtained in both cases, as confirmed by the X-ray diffraction patterns shown in Fig. 2. The alcohol acts as a homogenising agent since it is a mutual solvent for both the alkoxide and water, the latter either chemically bound to the nitrate salts or present in the technical ethanol. With the presence of ethanol as homogenising

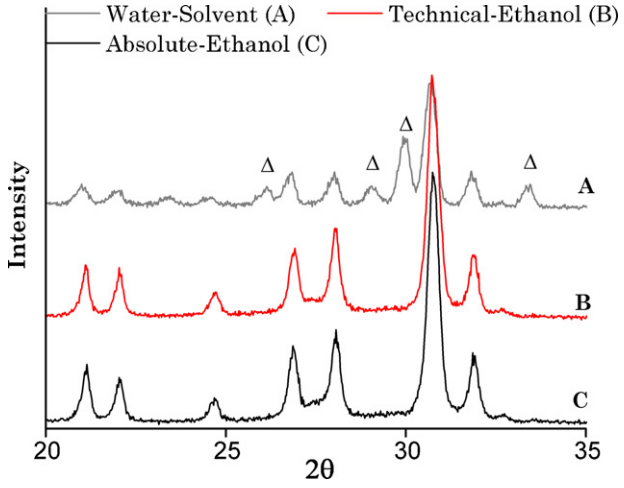

Fig. 2. Influence of the various solvent on the phase purity of the prepared powders. The presences of secondary phases (La_2O_3 indicated by open triangle) in the LASO-0 powder, prepared with a water based La-nitrate solution, is shown in the top XRD spectrum.

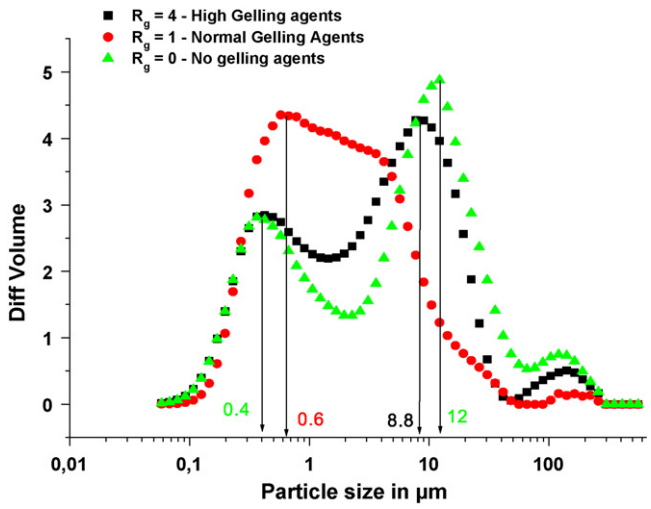

Fig. 3. Particle size distribution of the LASO-0 powder (as calcined) prepared with different ratio of gelling agents.

agent, the mixing of the alkoxide and water is improved so that hydrolysis, the first reaction step during sol formation,[26] is facilitated due to the miscibility of the alkoxide and water. However, the obtained particle size was strongly influenced by the type of ethanol that was used. In case technical ethanol, containing 3 vol% of ether in addition to water, was used, lower calcination temperatures were needed, resulting in the production of powders with a smaller particle size.

The additional ether from the technical ethanol helps in the formation of a more porous structure, which facilitates the easier removal of organics during calcination.[27,28] Hence most of the organics and nitrates are all removed at 900 °C. It is known that in the absence of ether moieties a non-porous gel is formed, causing the presence of a black residue after calcination at 900 °C, due to entrapment of residual carbon.[27] Increasing the calcination temperature to 1000 °C helps in removing the trapped carbon but at the same time results in the formation of harder agglomerates due to initial necking between the individual particles. Hence all the powder compositions reported in this paper were prepared as shown in the flow chart (Fig. 1).

3.1.1. *Influence of the ratio of gelling agents*

The ratio of gelling agents (R_g) was varied from zero (no gelling agents) to a value of 4. Again, the LASO-0 composition prepared with technical ethanol was chosen to study the influence of the gelling agents. The procedure used for making the gels was the same as before (Fig. 1). It was observed that phase pure compositions were formed irrespective of the R_g value.

When no gelling agents were used in the powder preparation, gellation occurred after leaving the sol at 70 °C for 6 h. The gel after calcination at 900 °C was found to be phase pure. However, the calcined powder was strongly agglomerated. When the R_g value was increased to a value of 1, the gel formed in less than 4 h when left at 70 °C. Calcination of the gel resulted in phase pure powder which consisted of softer agglomerates. Increasing the R_g value to 4 did not cause any considerable reduction in the time required for gellation. The gels on calcination resulted

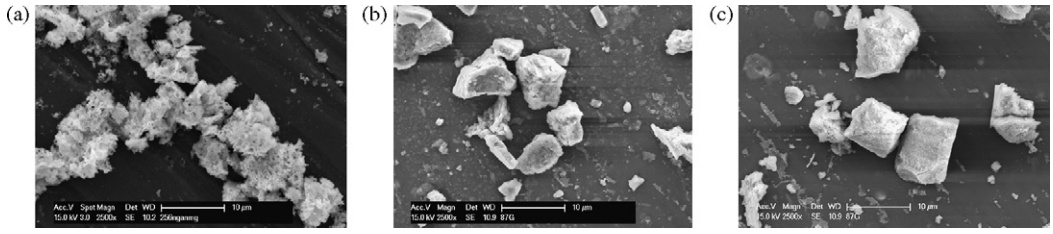

Fig. 4. Secondary electron (SE) images of the LASO-0 powder prepared with (a) normal amount ($R_g = 1$), (b) high amount ($R_g = 4$) and (c) no ($R_g = 0$) gelling agents.

Table 1
Influence of the ratio of gelling agent to metal ions (R_g) on the particle and crystallite size of the prepared LASO-0 powders.

R_g	Crystallite size (nm)	Particle size (μm)
0	139.8	0.4, 8.8
1	69.8	0.6
4	69.8	0.4, 12

in phase pure, but strongly agglomerated powder. Particle size measurements were performed on each of the powder batches, as shown in Fig. 3. Secondary electron images of the powders with different R_g values are shown in Fig. 4.

The crystallite size measurements are given in Table 1. Though the crystallite size is the same in the case of $R_g = 1$ and 4, the agglomerate size is larger as indicated by the particle size measurements, hereby confirming the fact that the latter powder consisted of strong agglomerates after calcination. A. Campero et al. state that a complex esterification reaction between EG and CA provides in situ water formation that can be used for the hydrolysis of TEOS, the oxide network former.[29] Since the reaction is absent when $R_g = 0$, longer gelling times are to be expected for that composition, which has indeed been observed.

The key advantage of the present synthesis technique being that there is no need for pH control for all the reported compositions and that no precipitation is observed. The time required for gelation can be reduced and overnight gelation times, as reported in most sol–gel processes,[19] are not required.

3.2. Powder characterization studies

It is evident from the thermogravimetric analysis, summarized in Fig. 5 and Table 2 that most of the organics and nitrates used in the preparation are removed at 900 °C and there is negligible weight loss when the temperature is further increased to 1000 °C. Most of the organics leave the gel in the temperature range between 80 and 200 °C. The decomposition temperature and evaporation temperature of most of the organics used in the powder preparation lie in this temperature range. The nitrates remain decomposing slowly during the rest of the heating process. No two step calcination process, as suggested in literature,[19] is needed as the powder obtained after calcination at 900 °C is already crystalline and all organics were eliminated. When higher calcination temperatures are used, the particles already start necking resulting in hard agglomerates and grain growth. This counteracts the densification step in a later stage, as will be described in Section 3.3.

Table 2 summarized the percentage weight loss that occurs in the temperature range from 800 up to 1000 °C. The maximum weight loss was less than 0.4 and 0.2% in the temperature range between 800–900 °C and 900–1000 °C, respectively. Hence, all gels were calcined at 900 °C for 8 h in order to obtain crystalline single-phase apatite type electrolyte powders. The X-ray powder diffraction patterns (Fig. 6) indicate all prepared powders are crystalline, they all crystallise in the apatite phase and no secondary phases are detected. The crystallite sizes of the powders were calculated using the *Scherrer* formula and the mean crystallite size for the powders was approximately 70 nm.[30]

The chemical compositions of the prepared powders were checked using the EDAX technique, coupled with the secondary electron (SE) images. Comparing the particle size measure-

Table 2
Percentage weight loss between different temperature ranges during TGA measurements (in oxygen up to a temperature of 1000 °C with an applied heating rate of 5 °C/min) performed on different gels with the indicated compositions.

S. no.	Composition	Weight change (%) (800–900 °C)	Weight change (%) (900–1000 °C)
1	LASO-0	0.3076	0.1250
2	LASO-1	0.3188	0.1178
3	LASO-2	0.3985	0.1043
4	LFSO	0.2892	0.1481
5	LSO	0.1875	0.0695

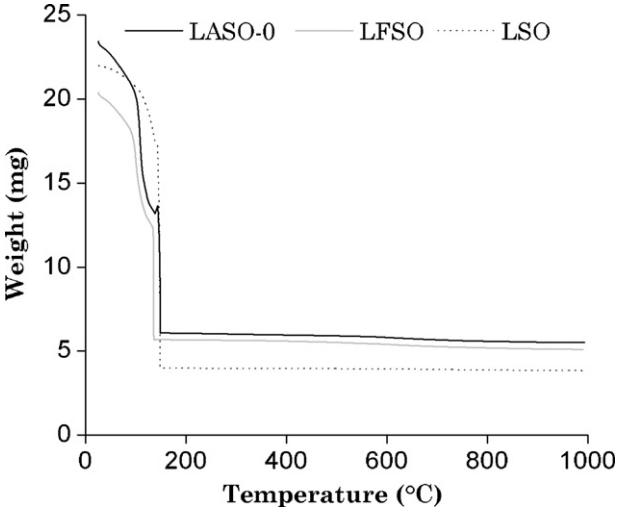

Fig. 5. Thermogravimetric analysis (TGA—in oxygen flowing rate 100 ml/min up to 1000 °C with a heating rate of 5 °C/min) curves for gels with LASO-0, LSO and LFSO compositions.

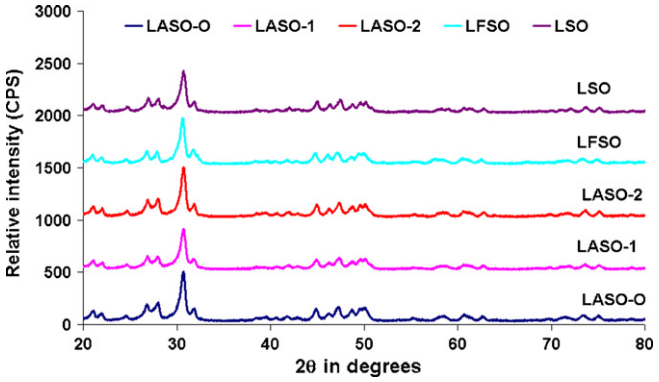

Fig. 6. X-ray diffraction (using Cu-Kα radiation (40 kV to 40 mA) with a 2θ range of 20–80° using the step size of 0.02° and an acquisition time of 2 s) of the investigated five compositions prepared by Pechini process after calcination at 900 °C for 8 h.

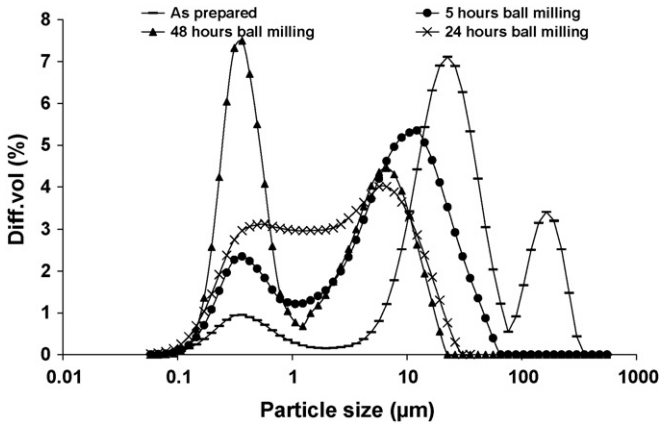

Fig. 8. Particle size distribution of LASO-0 powder as a function of milling time.

ments, performed on the powders just after calcination using a light diffraction technique, with the crystallite sizes obtained by X-ray diffraction, it is clear that the calcined powders are highly agglomerated, which is confirmed by the SE images shown in Fig. 7.

The calcined powders were ball milled in a multi-directional mixer to break up the agglomerates using zirconia milling balls. Technical ethanol was used as the milling medium. The ratio of milling balls to powder was maintained at 3:1. After 48 h of milling the particle size was measured using the Mastersizer equipment and SE images were taken. Both revealed that the average agglomerate size had decreased significantly after the milling procedure.

The evolution of the particle size as a function of the milling time is shown in Fig. 8. The SE images of all the powders prepared after the milling process are shown in Fig. 9. It is clear that the crystallite size of the synthesised powders lies within the nanometer (<100 nm) range, but that strong agglomeration occurs and that a milling step is essential to break up the agglomerates. The milling step will prove to be crucial for lowering the sintering temperature required to process fully dense compacts, as will be shown in the next paragraph.

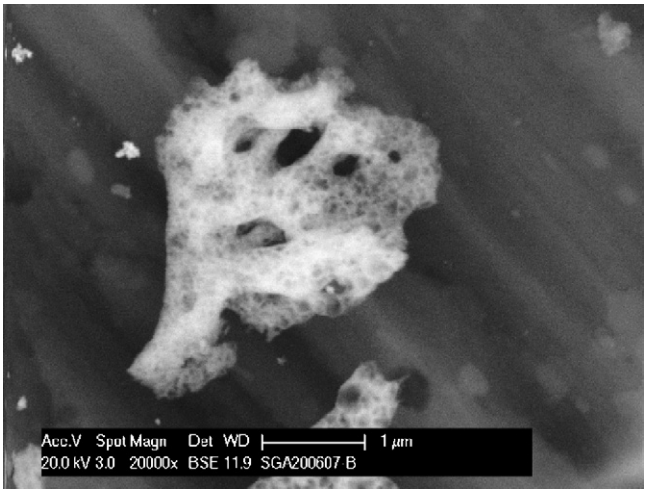

Fig. 7. Secondary electron image of LASO powder after calcination at 900 °C for 8 h.

3.3. Sintering studies

Pellets made from the milled and sieved powder were subjected to a dilatometer test to assess both the onset temperature of densification and to study the densification behaviour. The samples were heated up to 1600 °C at a rate of 3 °C/min in air. The results are summarized in Fig. 10. It is clear from the graph that the onset of densification (>1400 °C) is substantially higher when the lanthanum silicate is doped with aluminium.

The primary advantages of sol–gel or modified sol–gel techniques are the low temperature synthesis of a powder with homogeneous composition after calcination and a very small crystallite size that should enhance densification. The fine size of the powder helps in reducing the sintering temperature required to sinter it to full density. This helps in overcoming the sintering problem associated with aluminium-containing lanthanum silicates.

Green powder compacts with a diameter and height of 10 mm were uniaxially pressed from the different synthesised powder batches applying a pressure of 75 MPa. The obtained pellets were subsequently cold isostatically pressed (CIP) at 300 MPa. The relative green densities of the pellets after CIP were in the 38–42% range and were subsequently sintered in a resistively heated furnace (Nabertherm, Germany) in air within the 1400–1550 °C temperature range, while fixing the dwell time at the sintering temperature at 5 h. The obtained relative densities as function of sintering temperature and oxyapatite composition are represented in Fig. 11.

Relative density values greater than 96% were obtained after 5 h at 1550 °C for the LASO-0, LASO-1 and LASO-2 grades and after 5 h at 1500 °C for the LFSO and LSO grades. Fig. 12 shows representative SE micrographs of all the sintered samples after thermal etching at 1300 °C for 60 min in air.

The shrinkage curves, shown in Fig. 10, indicate that the temperature required for the onset of densification is greater for powders doped with aluminium (decreasing with decreasing aluminium content) and least for the undoped lanthanum silicate.

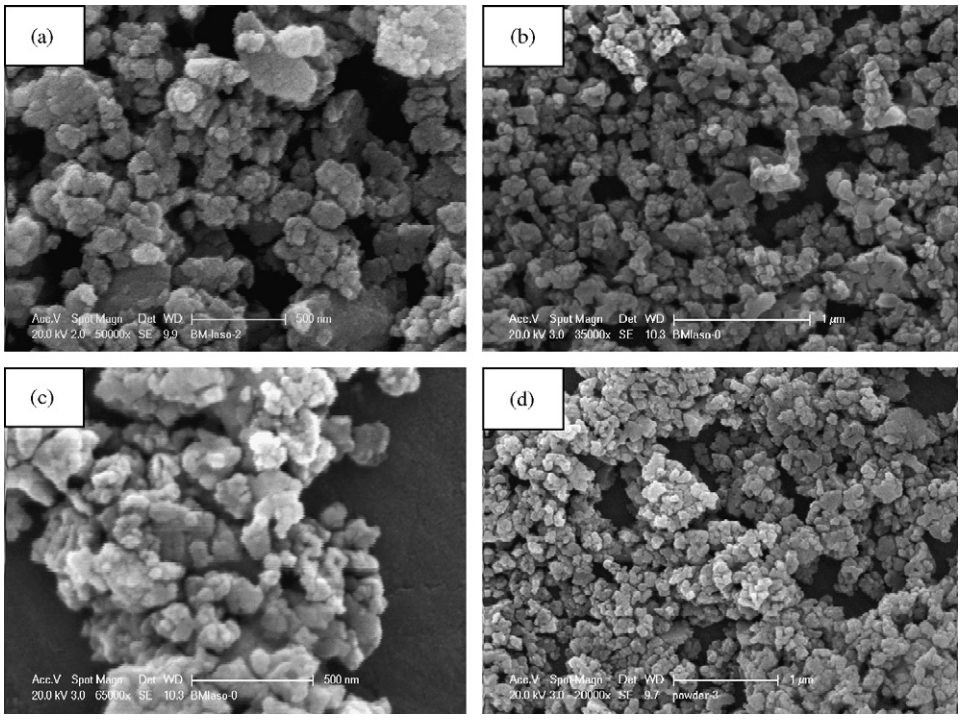

Fig. 9. Representative secondary electron images of all the prepared starting powders with different compositions, as prepared using the modified sol–gel process: (a) LASO-0, (b) LSO, (c) LFSO and (d) LASO-1.

In the case of undoped lanthanum silicates (LSO) the relative density values are greater than 90% at 1400 °C and increasing the sintering temperature results in microstructural coarsening and appearance of intergranular porosity (Fig. 12d). The shrinkage curves indicate clearly that, as the aluminium content increases, the temperature needed for sintering becomes higher. As reported in literature,[8] doping of iron has helped in reducing the sintering temperature of apatite type lanthanum silicates.

The sintering temperature and time reported in the present work is substantially lower than those reported in the literature. Sintering temperature ≥1600 °C with dwell times greater than 5 h have been reported[19–21,23,31] for solid-state synthesised LASO-0, LFSO and LSO powders. While, sol–gel prepared LSO[15] composition required sintering temperatures greater than 1600 °C for achieving density value close to 85%. The reduction in the particle size and the low calcination temperatures used aid in reducing the sintering temperature and time. In the case of the undoped lanthanum silicate, the sintering temperature and time are lower in comparison to solid-state synthesised powders and powders prepared using alternative low tempera-

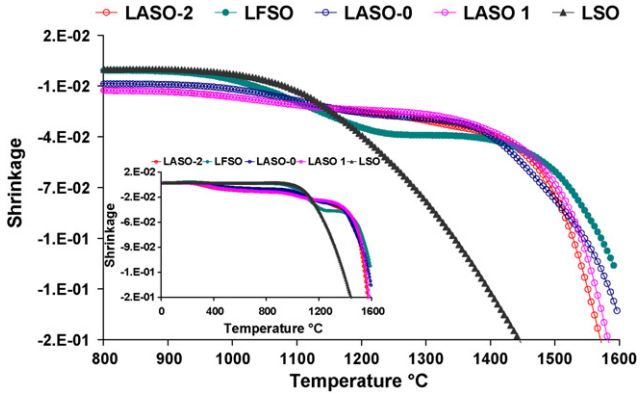

Fig. 10. Dilatometer curves (up to 1600 °C with a heating rate of 3 °C/min) for all powder composition.

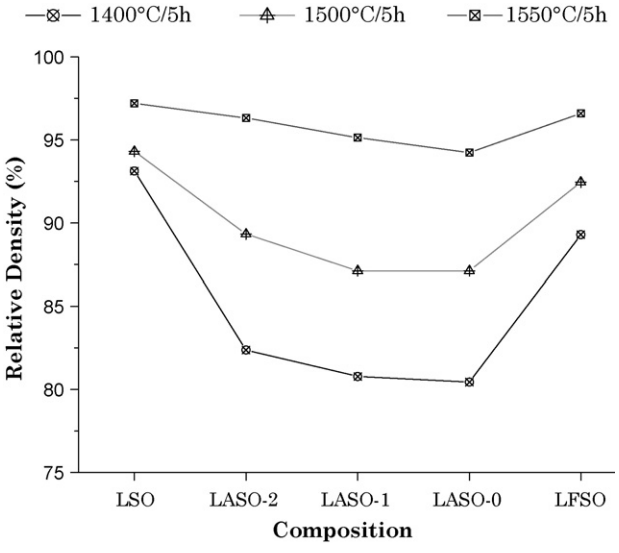

Fig. 11. Relative density evolution of pressureless sintered pellets as function of the sintering temperature and time for all the investigated composition (theoretical density of aluminium, iron and undoped apatites were taken as 5.45, 5.55 and 5.33 g/cm^3 respectively).

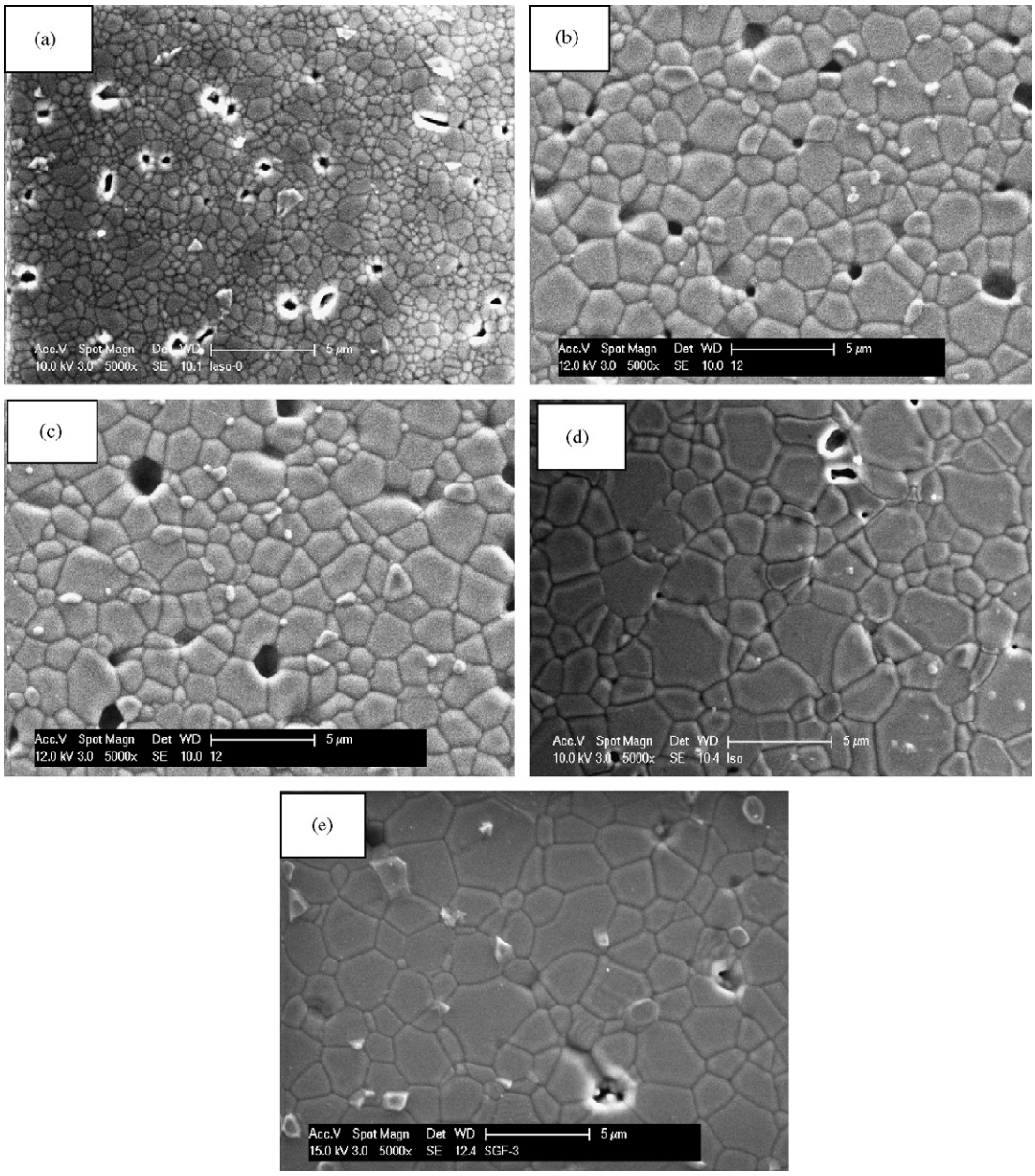

Fig. 12. Representative secondary electron images of pressureless sintered oxyapatite materials, as prepared from the different powder compositions: (a) LASO-0 (b) LASO-1 (c) LASO-2 ((a), (b) and (c) 1550 °C—5 h) (d) LSO and (e) LFSO ((d) and (e) 1500 °C—5 h).

ture methods.[7,8,10,12,15,17] The obtained density value for this composition, however, is lower when compared with the work of Ceĭleĭrier et al.,[12] who obtained compacts of undoped lanthanum silicate with a relative density of 92% after pressureless sintering at 1400 °C for 2 h, after using an intermediate attritor milling step.

4. Conclusions

Nano-crystalline rare earth oxyapatite powders of varying composition and dopant contents have been synthesised using a modified sol gel process. Single-phase nanostructured electrolyte powders were successfully synthesised using this low temperature, fast and user-friendly processing technique. Thermogravimetric analyses have shown that all organics are removed at 900 °C and hence no two step calcination is required. At the end of the single step calcination loosely aggregated, phase pure crystalline oxide nanopowders were obtained. It is observed that the nature of the solvents and the amount of gelling agents used, have a significant influence on the crystallite and agglomerate size of the final powders. The sintering behaviour of all the powders has been investigated and it is observed that substituting silicon with aluminium or iron delays the onset of densification and that the effect becomes more pronounced as the aluminium content increases. The reduced particle size of the starting powders, resulting from the optimized powder synthesis

conditions, helps in reducing the sintering temperature required to produce fully dense electrolyte materials that are essential for SOFC applications.

Acknowledgements

This work was performed within the EC 6 Framework Program (MATSILC-STRP 033410), the research fund of K.U. Leuven project GOA/08/007, and FWO project number 3E060133. K. Vanmeensel thanks the Fund for Scientific Research Flanders (FWO). The authors also acknowledge the support of the Belgian Federal Science Policy Office (BELSPO) through the NACER project (contract P2/00/07).

References

1. Yamamoto O. Solid oxide fuel cells: fundamental aspects and prospects. *Electrochim Acta* 2000;**45**(15–16):2423–35.
2. Panteix PJ, Julien I, Bernache-Assollant D, Abelard P. Synthesis and characterization of oxide ion conductors with apatite structure for intermediate temperature SOFC. *Mater Chem Phys* 2006;**95**:313–20.
3. Béchade E, Julien I, Iwata T, Masson O, Thomas P, Champion E, et al. Synthesis of lanthanum silicate oxyapatite materials as a solid oxide fuel cell electrolyte. *J Eur Ceram Soc* 2008;**28**:2717–24.
4. Nakayama S, Aono H, Sadaoka Y. Ionic conductivity of Ln_{10} $(SiO_4)_6O_3$ (Ln = La, Nd, Sm, Gd and Dy). *Chem Lett* 1995;**24**:431–2.
5. Nakayama S, Sakamoto M. Electrical properties of new type high oxide ionic conductor RE10Si6027 (RE = La, Pr, Nd, Sm, Gd, Dy). *J Eur Ceram Soc* 1998;**18**:1413–8.
6. Kendrick E, Saiful Islam M, Slater PR. Developing apatites for solid oxide fuel cells: Insight into structural, transport and doping properties. *J Mater Chem* 2007;**17**:3104–11.
7. Sansom JEH, Richings D, Slater PR. A powder neutron diffraction study of the oxide-ion-conducting apatite-type phases $La_{9.33}Si_6O_{26}$ and $La_8Sr_2Si_6O_{26}$. *Solid State Ionics* 2001;**139**:205–10.
8. McFarlane J, Barth S, Swaffer M, Sansom JEH, Slater PR. Synthesis and conductivities of the apatite-type systems, $La_{9.33+x}Si_{6-y}M_yO_{26+z}$ (M = Co, Fe, Mn) and $La_8Mn_2Si_6O_{26}$. *Ionics* 2002;**8**:149–54.
9. Rodrıguez-Reyna E, Fuentesa AF, Maczkab M, Hanuzab J, Boulahyad K, Amadore U. Facile synthesis, characterization and electrical properties of apatite-type lanthanum germanates. *Solid State Sci* 2006;**8**:168–77.
10. Tao S, Irvine JTS. Preparation and characterisation of apatite-type lanthanum silicates by a sol–gel process. *Mater Res Bull* 2001;**3**:1245–58.
11. Ceĭleĭrier S, Laberty C, Ansart F, Lenormand P, Stevens P. New chemical route based on sol–gel process for the synthesis of oxyapatite. *Adv Mater* 2006;**18**:615–8.
12. Ceĭleĭrier S, Laberty C, Ansart F, Lenormand P, Stevens P. New chemical route based on sol–gel process for the synthesis of oxyapatite $La_{9.33}Si_6O_{26}$. *Ceram Int* 2006;**32**:271–6.
13. Rodríguez-Reyna E, Fuentes AF, Maczka M, Hanuza J, Boulahya K, Amador U. Structural, microstructural and vibrational characterization of apatite-type lanthanum silicates prepared by mechanical milling. *J Solid State Chem* 2006;**179**:522–31.
14. Takashi N, Keishi N, Tadashi I, Toshio T. Preparation and electrical properties of $Ln_x(SiO_4)_6O_{(1.5x-12)}$ (Ln: Nd, La) with apatite structure. *J Sol–Gel Sci Technol* 2005;**33**:107–11.
15. Yoshioka H. Oxide ionic conductivity of apatite-type lanthanum silicates. *J Alloys Compd* 2006;**408–412**:649–52.
16. Masubuchi Y, Higuchi M, Takeda T, Kikkawa S. Preparation of apatite-type $La_{9.33}(SiO_4)_6O_2$ oxide ion conductor by alcoxide-hydrolysis. *J Alloys Compd* 2006;**408–412**:641–4.
17. Chesnaud A, Bogicevic C, Karolak F, Estournes C, Dezanneau G. Preparation of transparent oxyapatite ceramics by combined use of freeze-drying and spark-plasma sintering. *Chem Commun* 2007;**15**:1550–2.
18. Abram EJ, Sinclair DC, West AR. A novel enhancement of ionic conductivity in the cation-deficient apatite $La_{9.33}(SiO_4)_6O_2$. *J Mater Chem* 2001;**11**:978–1979.
19. Takeda N, Itagaki Y, Sadaoka Y. Relationship between pre-exponential factor and activation energy of conductivity in sintered $Ln_{9.33+x/3}Si_{6-x}M_xO_{26}$ (Ln = La, Nd, Sm, M = Al, Gd) with apatite-like structure. *J Ceram Soc Japan* 2007;**115**(10):643–7.
20. Tsipis EV, Kharton VV, Frade JR. Electrochemical behavior of mixed-conducting oxide cathodes in contact with apatite-type $La_{10}Si_5AlO_{26.5}$ electrolyte. *Electrochim Acta* 2007;**52**(13):4428–35.
21. Shaula AL, Kharton VV, Marques FMB. Oxygen ionic and electronic transport in apatite-type $La_{10-x}(Si,Al)_6O_{26\pm d}$. *J Sol State Chem* 2005;**178**:2056–61.
22. Shaula AL, Kharton VV, Waerenborgh JC, Rojas DP, Tsipis EV, Vyshatko NP, et al. Transport properties and Mossbauer spectra of Fe-substituted $La_{10-x}(Si,Al)_6O_{26}$ apatites. *Mater Res Bull* 2004;**39**:763–73.
23. Yoshioka H. Enhancement of ionic conductivity of apatite-type lanthanum silicates doped with cations. *J Am Ceram Soc* 2007;**90**(10):3099–105.
24. Kharton VV, Shaula AL, Patrakeev MV, Waerenborgh JC, Rojas DP, Vyshatko NP, et al. Oxygen ionic and electronic transport in apatite-type solid electrolytes. *J Electrochem Soc* 2004;**151**(8):1236–46.
25. Kharlamova T, Pavlova S, Sadykov V, Lapina O, Khabibulin D, Krieger T, et al. Low-temperature synthesis methods of doped apatite-type lanthanum silicates. *J Chem Eng Japan* 2007;**40**(13):1187–91.
26. Brinker CJ. Hydrolysis and condensation of silicates: effect on structure. *J Non-Cryst Solids* 1988;**100**:31–50.
27. Higuchi T, Kurumada K, Nagamine S, Lothongkum AW, Tanigaki M. Effect of addition of polymeric species with ether moieties on porous structure of silica prepared by sol–gel method. *J Mater Sci* 2000;**35**:3237–43.
28. Mizukami F, Maeda K, Toba M, Sano T, Niwa SI, Miyazaki M, et al. Effect of organic ligands used in sol–gel process on the formation of mullite. *J Sol–gel Sci Technol* 1997;**8**(101–106):101–6.
29. Campero A, Cardaso J, Pacheco S. Ethylene glycol-citric acid-silica hybrid organic-inorganic materials obtained by the sol–gel method. *J Sol–Gel Sci Technol* 1997;**8**:535–9.
30. Pleshko N, Boskey A, Mendelsohn R. Novel infrared spectroscopic method for the determination of crystallinity of hydroxyapatite minerals. *Biophys J* 1991;**60**:786–93.
31. Gorshkov MYu, Neuimin AD, Bogdanovich NM, Bronin DI. Electroconductivity and transport numbers of solid electrolytes $La_{10-x}Ca_xA_6O_{27-\delta}$ and $La_{9.33+\delta}A_{6-x}Al_xO_{26}$ (A = Si, Ge) with apatite structure. *Russ J Electrochem* 2006;**42**:7737–43.